



REPURPOSING DONEPEZIL AS A POTENTIAL ZIKA VIRUS INHIBITOR: A SYSTEMATIC VIRTUAL SCREENING AND MOLECULAR DOCKING APPROACH

AMAKU JAMES FRIDAY¹, BUHARI MAGAJI² AND TOBBY CASSANDRA ONYEKACHI¹

¹Department of Chemistry, Michael Okpara University of Agriculture, Umudike

²Department of Chemistry, Faculty of Science, Gombe State University

Corresponding email: amakufj2006@gmail.com

ABSTRACT

A potential global threat of Zika virus (ZKV) as observed in February 2016 in Brazil has called for intensive surveillance and proactive measures to ensure its spread and re-emergence are nipped. However, clinically approved drugs for dengue have shown insufficient capacity in curbing ZKV. Hence, a systematic repurposing of drug with alien therapeutic implication *via* the ligand-based virtual screening approach may proffer a path to finding drugs with potential to inhibit ZKV. Compounds retrieved from the ZINC database were docked with 5Y6N protein by making use of AutoDockVina tools. In silico prediction of pharmacokinetic properties and quantum chemical calculations of The best hit were assessed. The best five drug-like compounds were identified and among these five compounds, ZINC84071344 (*N*-(2-fluoro-5-nitrophenyl)-6-methoxypicolinamide) was found to interact best with 5Y6N protein with a binding energy of – 6.6 kcal/mol and the formation of H-bonds with LYS 200, GLY 199 and ARG 462 amino acid residues. The lead molecule (ZINC84071344) exhibit the tendency to possess high physicochemical and ADME properties for an oral drug. A further experimental assessment of ZINC84071344 could lead to the discovery of novel inhibitor of 5Y6N protein.

Keywords: Zika virus, Virtual screening, Donepezil, Molecular docking

INTRODUCTION

Zika virus (ZKV) is an emerging human-pathogenic illness with the capacity to cause a matchless large-scale global epidemic (Chan *et al.*, 2017). This virus is spherical and belongs to *Flaviviridae* family. It is a member of the *spodweni* serocomplex of the *flavivirus* genus (Faye *et al.*, 2014; Haddow *et al.*, 2012). It was found that besides transmission *via* mosquito bites, ZKV can also be acquired through blood transfusion, unprotected sex, perinatal and congenital

transmission (Foy *et al.*, 2011). At first, ZKV was thought to be a self-limiting infection that may pose little or no threat to human, however, it turned out to have unleashed devastating health challenges among which are chronic hepatic dysfunction, shock, severe neurological defects such as Guillain-Barré syndrome (GBS), meningoencephalitis and myelitis, acute respiratory distress syndrome, thrombocytopenia and disseminated intravascular coagulation with hemorrhagic complications, multiorgan

failure and death (Brito, 2016; Shapshak, Sinnott, Somboonwit, & Kuhn, 2015). Besides the aforementioned implications, studies on hematospermia and mouse models of orchitis speculate long-term negative implication on male fertility (Chan *et al.*, 2016; Foy *et al.*, 2011; Govero *et al.*, 2016; Ma *et al.*, 2016). The major threat of ZKV to human is its proclivity to central nervous system (CNS) disorder and prenatal infection such as retarded fetal growth, neurological and ocular aberrations, intracranial calcification and in certain situation may lead to perinatal death (Chibueze *et al.*, 2017; Singh *et al.*, 2016). Meanwhile, symptoms connected to ZKV infected patient include malaise, fever, arthralgia, mild headache, swollen lymph nodes, joint pains, conjunctivitis and rashes (Sahoo, Lingaraja Jena, & Kumar, 2016).

Ever since the emergence of ZKV in 1947 *via* its isolation from the Rhesus 766 monkey in the Zika forest of Uganda (Faye *et al.*, 2014), the spread of ZKV have been reported in countries such as Tanzania, Egypt, Gabon, Central African Republic, Sierra Leone, India, Malaysia, Philippines, Thailand, Vietnam and Indonesia (Hayes, 2009; Shawan *et al.*, 2015). In 2015, a devastating out-brake of ZKV was also reported in Brazil (Campos, Bandeira, & Sardi, 2015). Zika virus is composed of a unit stranded, positive sense and 11-kb RNA which functions as mRNA for the synthesis of polyprotein precursor and as a template for genome replication in the cytoplasm of the host cell (Aleshin, Shiryaev, Strongin, & Liddington, 2007). Structural assay of ZKV showed that the genome encodes three structural proteins

(capsid (c), envelope (E) and pre-membrane/membrane (prM)) found in the mature virion and seven nonstructural (NS) proteins which include NS1, NS2A, NS2B, NS3, NS4A, NS4B and NS5 (Chambers *et al.*, 1990). It is worth mentioning that, the aforementioned nonstructural proteins of ZKV are not part of the virion architecture (Yuan *et al.*, 2017). However, NS3 and NS5 proteins play a cardinal role, as they collectively anchor most of the catalytic activities necessary for capping and replication processes (Wu, Wang, Sun, Hu, & Syu, 2003).

At this point it is 'sad' to say that there is no medication that can match the strength of this pathogenic virus, this could be due to the complexity of the virus. Meanwhile, it is currently managed *via* the intake of fluids, observing enough rest supported with the use of antipyretics and analgesics (Duffy *et al.*, 2009). In a bid to arrest the spread of ZKV, intensive research has been tailored towards screening drug libraries using cell culture-based antiviral analyses (Yuan *et al.*, 2017). Unfortunately, the *in vitro* analysis of drug libraries revealed some clinically approved anti-cancer drugs that possess anti-ZKV activity, but due to the unknown negative health implications of these drugs, the application of these drugs as treatment for ZKV infected persons are not encouraged (Yuan *et al.*, 2017). Structure-based virtual screening (SBVS) is an effective approach to detects potential beneficial binding affinities of ligands into the specific active binding site. The SBVS approach gives assess to understanding the nature of the active site and the protein-ligand interactions (Kumalo &

Soliman, 2016). On the contrary, Ligand-based virtual screening technique is often employed to systematically generates libraries of compounds based on the knowledge of a molecule (Cele, Ramesh, & Soliman, 2016). Recent study revealed that ZKV target neuronal cells (Millichap, 2016; Miner & Diamond, 2016; Mlakar *et al.*, 2016; Tang *et al.*, 2016). Hence, it is envisioned that repurposing clinically approved drugs (donepezil) designed to treat neurological disorder for a systematic Ligand-based virtual screening could be an alternative approach to discovering new ZKV inhibitors.

MATERIAL AND METHODS

System Preparation

The 3D structure of ZIKA virus protein in complex with adenosine-5'-diphosphate (ADP) was retrieved from the Research Collaboratory for Structural Bioinformatics Protein Data Bank (RCSB-PDB) with ID 5Y6N. The structure of ZKV virus was a distinct single chains complexed with a complementary metal residue residue (Mn^{2+}) and ADP. The preparation of the receptor acquired from the protein data bank was performed by making use of UCSF Chimera interface, in which hydrogens were added to the protein (5Y6N) and removed from the ligand prior to molecular docking step (Pettersen *et al.*, 2004).

Pharmacophore Generation

The pharmacophore model of donepezil was retrieved from drugbank online platform. The constructed model was added to ZINCPharmer with a unique

criteria (Koes & Camacho, 2012; Morris *et al.*, 1998; Pettersen *et al.*, 2004).

Structure-Based Virtual Screening

The virtual screening technique was used to identify potential inhibitors with pharmacophoric characteristics similar to donepezil from a large database of drug-like compounds. The constructed model was added to ZINCPharmer with a distinct criteria (molecular weight of <500 Da, hydrogen bond donors <5, hydrogen bond acceptors <10 and rotatable bonds <6), to screen the ZINC database for the potential 5Y6N inhibitors (Koes & Camacho, 2012; Morris *et al.*, 1998; Pettersen *et al.*, 2004). Based on the generated pharmacophore (donepezil), the ZINC database was screened to obtain drug-like compounds with similar pharmacophoric features as exhibited by donepezil upon binding to 5Y6N.

Preparation of Potential 5Y6N Inhibitors

Possible potential inhibitors of 5Y6N proteins were retrieved in their 2D conformations from the ZINC database. Optimization was carried out for each of the compounds retrieved from ZINC database on Avogadro using the MMF94 force field (Hanwell *et al.*, 2012). The minimized 3D structures of the acquired ligands were thereafter individually exported to UCSF Chimera for further preparation prior to molecular docking. Hydrogen atoms were removed and Gasteiger partial charges were allocated to the compounds.

Molecular Docking

Molecular docking was carried out on all the hits acquired from the ZINC database to predict their binding conformation and

affinity within the active site region of 5Y6N. Docking was carried out by making use of the AutoDockVina software (Morris *et al.*, 1998). The grid box that defines the binding active site region of 5Y6N protein was estimated from the AutoDock Vina functionality on UCSF Chimera (Pettersen *et al.*, 2004). The grid box size and centre coordinates for the protein were x (8.35, 3.07), y (11.68, 63.55) and z (10.65, 66.47) respectively. Meanwhile, a maximum of 10 conformers were considered during the docking process.

In silico Prediction of Pharmacokinetic Properties

The best inhibitors (ZINC84071344) among the virtually screened pharmacophores was assessed for its pharmacokinetic properties using the online SwissADME tool (Daina *et al.*, 2017). This tool was also used to establish the drug-like qualities of ZINC84071344. To achieve this, the molecular weight, logP value, number of hydrogen bond donors and acceptors of ZINC84071344 were taken into consideration.

Quantum Chemical Calculations

The quantum chemical calculations were carried out on Gaussian 09 equipped with Gaussview 5.0 program by making use of DFT (B3LYP) methods with 6-311++G (d, p) basis sets. Electronic transitions in the UV-Vis spectral region were calculated by time-dependent (TD) DFT method with B3LYP level and 6-311++G (d, p) basis set. The frontier molecular orbitals energies

(HOMO and LUMO energies) were also determined.

RESULTS

Intensive effort has been made in the search for a cure for ZIKA virus. The conventional approach to certify a molecule as a drug for a particular ailment is time-consuming and very expensive. Hence, the systematic approach to mining small molecules with therapeutic impact against pathogenic disease is imperative.

In this study, we sort to ‘unearth’ latent potential inhibitors of 5Y6N protein that could serve as an alternative to prevailing therapeutic options for ZKV. Based on the pharmacophoric features of donepezil as shown in Fig 1, ninety-nine models were generated *via* virtual screening on the ZINCpharmer compound. This led to the identification of ZINC84071344 as a molecule with the capacity to inhibit 5Y6N (see Table 1).

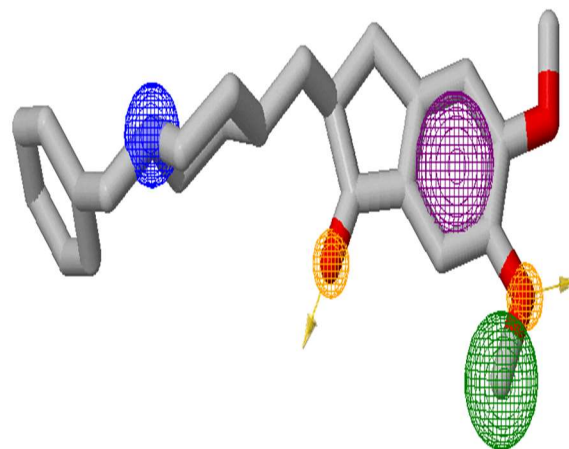
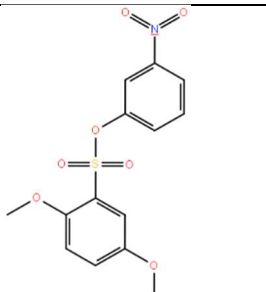
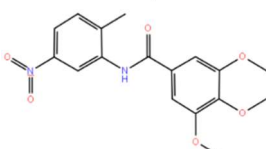


Figure 1: The 3D image of donepezil showing the pharmacophoric signals on the ZINCPharmer online Platform

Table 1: 2D structures of inhibitors (colored by heteroatoms) and their corresponding binding affinities from molecular docking.

S/N	ZINC CODE	STRUCTURE	SCORE * ΔG (Kcal/mol)
*	Donepezil ZINC84071344		-4.5
1			-6.6
2	ZINC63458398		-6.2
3	ZINC76016626		-6.1
4	ZINC90706747		-6.0

5	ZINC16091814		-5.8
6	ZINC00168706		-3.3

The interactions of the amino acid residues with the inhibitors within the pocket of the receptor reveal why the lead molecule may be more potent than daptomycin. Amino acids such as PRO 464, ASN 463, ASN 330, ARG 462, ARG 202, THR 201, LYS 200, GLY 199, ALA 198, GLY 197 and ASN 417 were frequently observed with the receptor pocket, this indicate similar site of interaction for all the ligangs under investigation.

The top five drug-like compounds obtained *via* molecular docking of the predicted ninety-three compounds against ZKV were reported as auspicious candidates for further analysis. The chemical structure of these five molecules showing their ligand-interactions in their complexed state with ZKV along with donepezil are displayed in Figure 2 to 7.

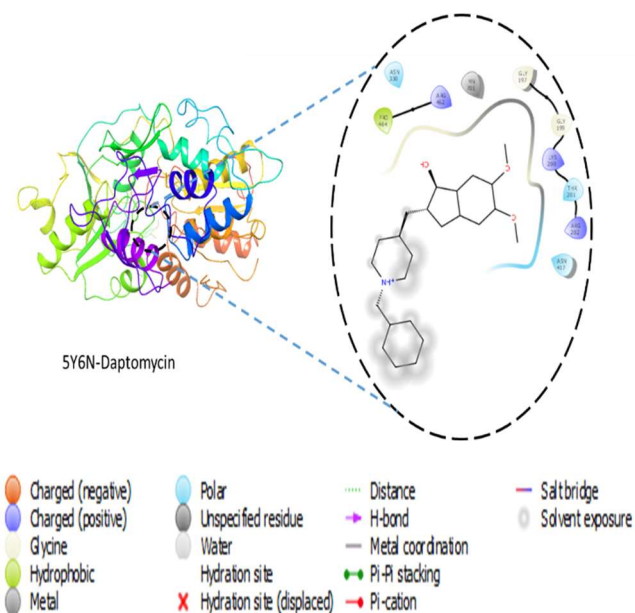


Figure 2: The 3D X-ray crystal structure of 5Y6N complex with donepezil showing also the binding site region and the residues that constitute this binding site region.

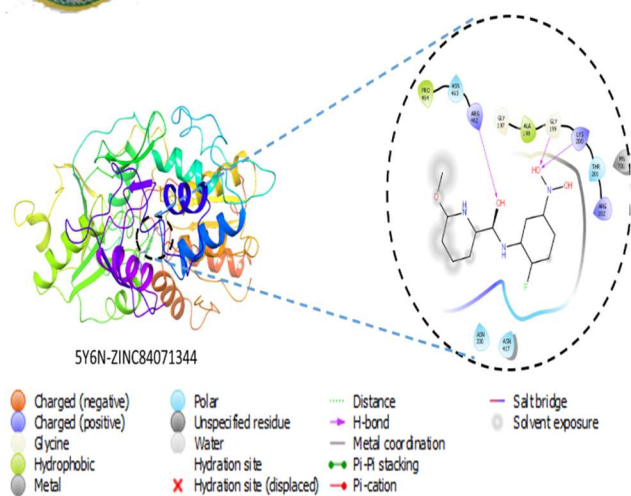


Figure 3: The 3D X-ray crystal structure of 5Y6N complex with ZINC84071344 showing also the binding site region and the residues that constitute this binding site region.

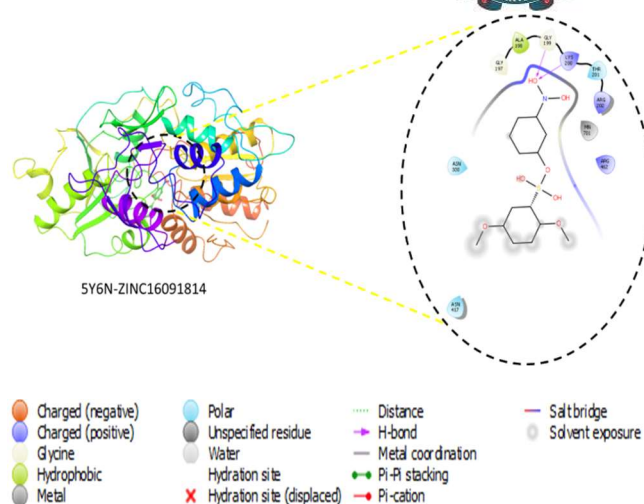


Figure 5: The 3D X-ray crystal structure of 5Y6N complex with ZINC16091814 showing also the binding site region and the residues that constitute this binding site region.

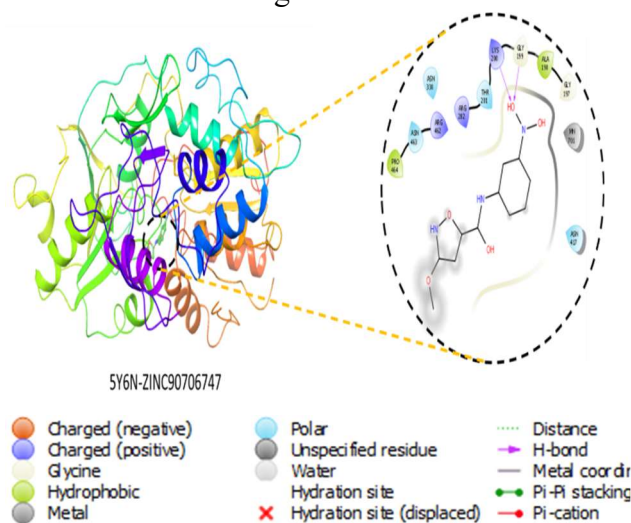


Figure 4: The 3D X-ray crystal structure of 5Y6N complex with ZINC90706747 showing also the binding site region and the residues that constitute this binding site region.

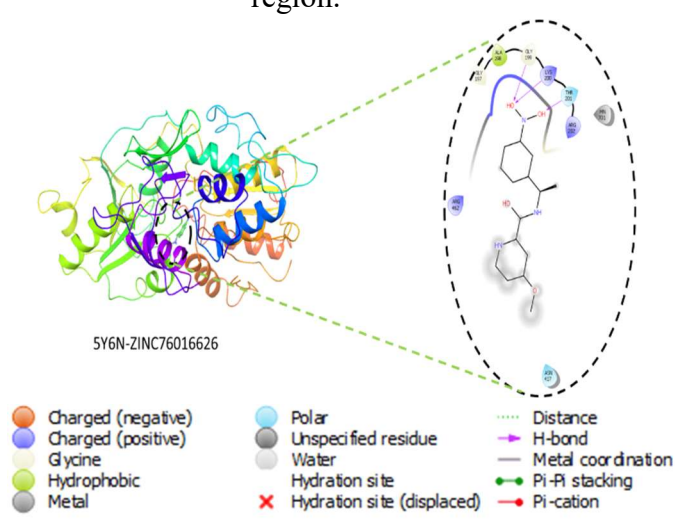


Figure 6: The 3D X-ray crystal structure of 5Y6N complex with ZINC76016626 showing also the binding site region and the residues that constitute this binding site region.

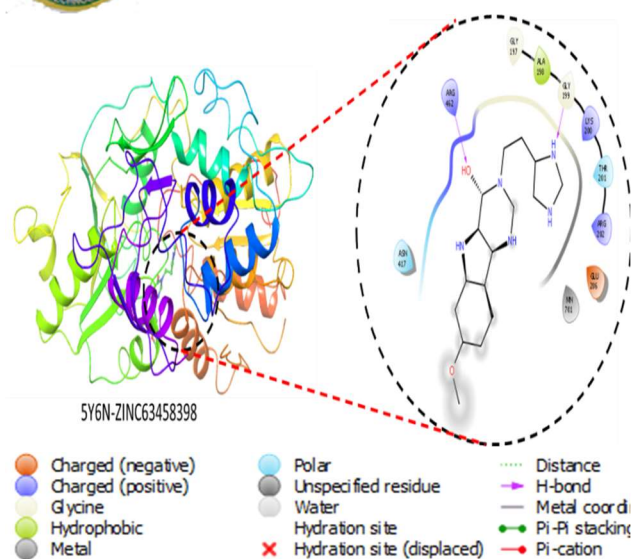


Figure 7: The 3D. X-ray crystal structure of 5Y6N complex with ZINC63458398 showing also the binding site region and the residues that constitute this binding site region.

The UV-VIS spectrum of the lead molecule (ZINC84071344) were also establish (Figure 9). In the present study the energy gap (ΔE) was estimated from LUMO minus HOMO energies value. Absolute electronegativity (χ), absolute hardness (η) and electrophilicity index (ω) of ZINC8471344 were computed by B3LYP/6-311++G(d,p) method and listed in Table 2. According to Koopmans' theorem, the ionization potential ($IP \approx -E_{HOMO}$) and electron affinity ($EA \approx -E_{LUMO}$) can be expressed through HOMO and LUMO orbital energies (Koopmans, 1934). Meanwhile, the electronegativity (χ) can be obtained from the average of the sum of ionization potential (IP) and electron affinity (EA) ($\chi = \frac{IP+EA}{2}$). The hardness (η) of a molecule is related to the gap between the HOMO and LUMO orbitals, however, the larger the HOMO-LUMO energy gap the

harder the molecule (Pandey, Muthu, & Gowda, 2017) (Figure 8), however, this descriptor is estimated from $(\eta) = \frac{IP-EA}{2}$.

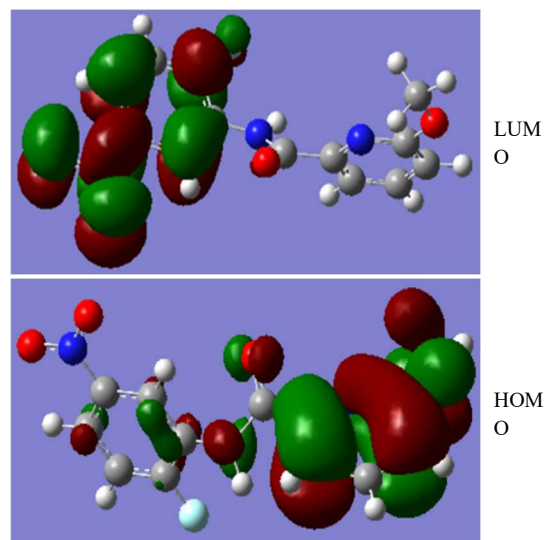


Figure 8: The 3D images of ZINC84071344 showing its HOMO and LUMO energies.

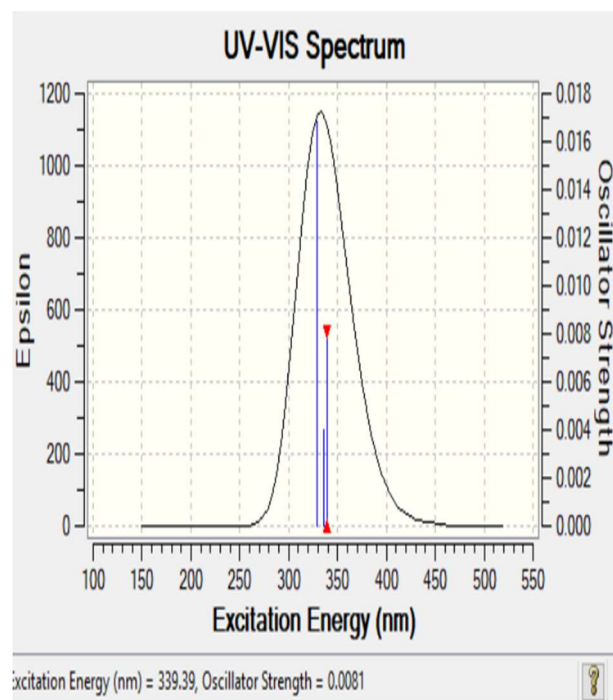


Figure 9: UV-VIS spectrum of ZINC84071344

The selected five lead molecules were also observed to impart a certain degree of inhibition on 5Y6N protein with enhanced binding energy as compared to donepezil. Thus, the higher binding affinity of the reported lead molecules compared to donepezil in their respective docked forms suggest that the proposed five molecules would probably bind more competitively in the pocket of 5Y6N protein (see Table 2). Hence, the lead molecule with the best inhibitory activity against 5Y6N brings science closer to defeating the spread of ZKV infections.

Table 2: HOMO-LUMO energies and calculated global reactivity parameters of ZINC84071344 molecule calculated by B3LYP/6-311++G (d,p) method.

Parameters	Theoretical values
E_{HOMO} (eV)	0.26021
E_{LUMO} (eV)	0.11075
$(E_{\text{LUMO}}(\text{eV}) - E_{\text{HOMO}}(\text{eV}))$	0.14075
Electronegativity (χ)	0.18548
Chemical hardness (η)	0.07473
Softness (S)	13.3820
Chemical potential	-0.07473
Electrophilicity index	0.037365

DISCUSSION

The pharmacophore model of donepezil was sourced from drug bank database. Meanwhile, the insufficient capacity of donepezil to inhibit ZIKAV demands a quick modification or replacement. To achieve this, virtual screening of the model (donepezil) was performed on ZINC database by making use of ZINCpharmer. This approach investigates smaller molecules with similar pharmacophoric fixture to donepezil. At the end of the search ninety-three chemical compounds

with similar pharmacophoric feature were predicted. Prior to searching step, the selected features were fixed on the ZINCpharmer such that the obtained molecules will obey the Lipinski's rule of five (molecular weight, not more than 500 Da; hydrogen bond donor not more than 5; hydrogen bond acceptors not more than 10; log p-value not greater than 5).

The top five drug-like compounds obtained *via* molecular docking of the predicted ninety-three compounds against ZKV were reported as auspicious candidates for further analysis. From the wide array of compounds complexed with ZKV, five molecules displayed great affinity for ZKV in the complexed forms but one among these five was observed to have the Highest binding energy.

The interactions of the predicted lead molecules with 5Y6N proteins were anchored on the formation of hydrogen bonds with active site residues of 5Y6N protein as clearly shown in the ligand interaction of the complexes. The model molecule (donepezil) showed no significant hydrogen-bond interaction with 5Y6N protein. This could be responsible for the poor binding activity of this molecule (-4.5 Kcal/mol). However, covalent interactions with the amino acid residues within the pocket of then 5Y6N protein was observed.

On the other hand, ZINC16091814 and ZINC90706747 had a binding affinity of -5.8 and 6.0 respectively. They were observed to bind with LYS 200 and GLY 199 amino acid residues. A slight increase in the binding affinity of ZINC76016626 was observed (-6.1 Kcal/mol), this could be due to the fact that

more amino acids residues interacted with this molecule (THR 201, LYS 200 and GLY 199). It was also found that the interaction of ZINC63458398 with 5YN6 protein resulted in a better binding affinity (-6.2 Kcal/mol), involving the ligand-interactions of GLY 199 and ARG 462 at the binding site. *N*-(2-fluoro-5-nitrophenyl)-6-methoxypicolinamide (ZINC84071344) having molecular weight of 291.23 g/mol showed the highest binding affinity of (-6.6 kcal/mol) and was observed to interact with active site residues of 5YN6 by forming hydrogen bonds with LYS 200, GLY 199 and ARG 462 (Figure 3).

Pharmacokinetic Assessment of Potential 5Y6N Protein Inhibitors

In a bid to assess the possibility of administering the predicted inhibitor to man, assessment of the biophysicochemical properties of the lead compounds becomes imperative. The online platform SwissADME was used to predict the pharmacokinetic properties of ZINC84071344. The predicted pharmacokinetic properties include Absorption, Distribution, Metabolism, Excretion (ADME) properties. Therefore, the *In silico* ADMET analysis of the lead compound is imperative. In performing this, the multiple screening step and the risk of late-stage attrition of drug development are reduced.

The lead compound (ZINC84071344) from this study has demonstrated promising pharmacokinetic properties. This assessment took into consideration the Lipinski's rule of five. Meanwhile, the ZINC84071344 was noticed to obey Lipinski's rule of five. In

addition to the properties of ZINC84071344, the membrane permeability of this compound was better understood from the lipophilicity (XlogP) score obtained from the *In silico* ADMET analysis. A lipophilicity of LogP >5, indicates a high a metabolic activities, decreased solubility and indigent oral absorption, also molecules with a logP greater than 1 or less than 4 ($1 < x < 4$) are known to exhibit the tendency to possess high physicochemical and ADME properties for an oral drug (Arnott & Planey, 2012; Wang *et al.*, 2015; Waring, 2010). As shown in Table S3, the lead molecule (ZINC84071344) have demonstrated good oral absorbance, high metabolic turnover and high solubility.

Toxicity of druglike molecules increases with increase in molecular weight compound. Apparently, the moderate molecular weight of the lead compound ($291.32 \text{ g mol}^{-1}$) present value-added benefit of the property of ZINC84071344 with regards to its application as 5Y6N protein inhibitor.

Global Reactivity Descriptors

With the aid of density functional theory (DFT), the global reactivity of the lead compound was estimated. To achieve this, the output of the estimated DFT parameters (Frontier molecular orbital (FMO) theory) were used to calculate reactivity descriptors such as Electronegativity (χ), hardness (η), softness (S) and electrophilicity index. In the present study the energy gap (ΔE) was estimated from LUMO minus HOMO energies value. Absolute electronegativity (χ), absolute hardness (η) and electrophilicity index (ω) of ZINC8471344 were computed

by B3LYP/6-311++G(d,p) method. According to Koopmans' theorem, the ionization potential ($IP \approx -E_{HOMO}$) and electron affinity ($EA \approx -E_{LUMO}$) can be expressed through HOMO and LUMO orbital energies (Koopmans, 1934). Meanwhile, the electronegativity (χ) can be obtained from the average of the sum of ionization potential (IP) and electron affinity (EA) ($\chi = \frac{IP+EA}{2}$). The hardness (η) of a molecule is related to the gap between the HOMO and LUMO orbitals, however, the larger the HOMO-LUMO energy gap the harder the molecule (Pandey et al., 2017), however, this descriptor is estimated from ($\eta = \frac{IP-EA}{2}$). In the same trend, the global softness of the lead compound is determined from the inverse of global hardness (Yang & Parr, 1985). Hence, softness = ($S = \frac{1}{\eta}$). The chemical potential of ZINC8471344 was also calculated from the average of electron affinity in combination with ionization energy ($\mu = -\frac{IP+E}{2}$). Finally, the electrophilicity index (ω) that suggest the tendency of the lead compound (ZINC8471344) to accept electrons was estimated by making use of the electronic chemical potential (μ) and chemical hardness (η) ($\omega = \frac{\mu^2}{2\eta}$). The outcome of the global reactivity assay shows that the ZKV inhibitor will readily interact with the 5Y6N protein.

CONCLUSION

This study proposes new compound (ZINC84071344) that have shown promising physicochemical properties and strong interactions with the formation of H-bonds

with LYS 200, GLY 199 and ARG 462 amino acid residues at the active binding site of 5Y6N protein. The pharmacokinetic investigation revealed this ZINC84071344 is satisfactory for use as oral absorbance, besides, its low molecular weight and less toxicity is an added value to the property of ZINC84071344. On the other hand, the global reactivity descriptors of the lead compound (ZINC84071344) estimated from the density functional theory calculations revealed the ease of ZINC84071344 interaction with 5Y6N protein. Apparently, ZINC84071344 has shown significant potential to inhibit 5Y6N protein and thus, further experimental investigation is necessary for its efficacy prior to synthesis.

REFERENCES

- Aleshin, A. E., Shiryayev, S. A., Strongin, A. Y., & Liddington, R. C. (2007). Structural evidence for regulation and specificity of flaviviral proteases and evolution of the Flaviviridae fold. *Protein science*, 16(5), 795-806.
- Arnott, J. A., & Planey, S. L. (2012). The influence of lipophilicity in drug discovery and design. *Expert Opinion on Drug Discovery*, 7(10), 863-875.
- Brito, C. (2016). Zika virus: a new chapter in the history of medicine. *Acta medica portuguesa*, 28(6), 679-680.
- Campos, G. S., Bandeira, A. C., & Sardi, S. I. (2015). Zika virus outbreak, bahia, brazil. *Emerging infectious diseases*, 21(10), 1885.
- Cele, F. N., Ramesh, M., & Soliman, M. E. (2016). Per-residue energy decomposition pharmacophore model

- to enhance virtual screening in drug discovery: a study for identification of reverse transcriptase inhibitors as potential anti-HIV agents. *Drug design, development and therapy*, 10, 1365.
- Chambers, T. J., Weir, R. C., Grakoui, A., McCourt, D. W., Bazan, J. F., Fletterick, R. J., & Rice, C. M. (1990). Evidence that the N-terminal domain of nonstructural protein NS3 from yellow fever virus is a serine protease responsible for site-specific cleavages in the viral polyprotein. *Proceedings of the National Academy of Sciences*, 87(22), 8898-8902.
- Chan, J. F.-W., Chik, K. K.-H., Yuan, S., Yip, C. C.-Y., Zhu, Z., Tee, K.-M., . . . Lu, G. (2017). Novel antiviral activity and mechanism of bromocriptine as a Zika virus NS2B-NS3 protease inhibitor. *Antiviral research*, 141, 29-37.
- Chan, J. F.-W., Zhang, A. J., Chan, C. C.-S., Yip, C. C.-Y., Mak, W. W.-N., Zhu, H., . . . Cai, J.-P. (2016). Zika virus infection in dexamethasone-immunosuppressed mice demonstrating disseminated infection with multi-organ involvement including orchitis effectively treated by recombinant type I interferons. *EBioMedicine*, 14, 112-122.
- Chibueze, E. C., Tirado, V., da Silva Lopes, K., Balogun, O. O., Takemoto, Y., Swa, T., . . . Menendez, C. (2017). Zika virus infection in pregnancy: a systematic review of disease course and complications. *Reproductive health*, 14(1), 28.
- Duffy, M. R., Chen, T.-H., Hancock, W. T., Powers, A. M., Kool, J. L., Lanciotti, R. S., . . . Dubray, C. (2009). Zika virus outbreak on Yap Island, federated states of Micronesia. *New England Journal of Medicine*, 360(24), 2536-2543.
- Faye, O., Freire, C. C., Iamarino, A., Faye, O., de Oliveira, J. V. C., Diallo, M., & Zanotto, P. M. (2014). Molecular evolution of Zika virus during its emergence in the 20th century. *PLoS neglected tropical diseases*, 8(1), e2636.
- Foy, B. D., Kobylinski, K. C., Foy, J. L. C., Blitvich, B. J., da Rosa, A. T., Haddock, A. D., . . . Tesh, R. B. (2011). Probable non-vector-borne transmission of Zika virus, Colorado, USA. *Emerging infectious diseases*, 17(5), 880.
- Govero, J., Esakky, P., Scheaffer, S. M., Fernandez, E., Drury, A., Platt, D. J., . . . Salazar, V. (2016). Zika virus infection damages the testes in mice. *Nature*, 540(7633), 438.
- Haddock, A. D., Schuh, A. J., Yasuda, C. Y., Kasper, M. R., Heang, V., Huy, R., . . . Weaver, S. C. (2012). Genetic characterization of Zika virus strains: geographic expansion of the Asian lineage. *PLoS neglected tropical diseases*, 6(2), e1477.
- Hanwell, M. D., Curtis, D. E., Loni, D. C., Vandermeersch, T., Zurek, E., & Hutchison, G. R. (2012). Avogadro: an advanced semantic chemical editor, visualization, and analysis

- platform. *Journal of cheminformatics*, 4(1), 17.
- Hayes, E. B. (2009). Zika virus outside Africa. *Emerging infectious diseases*, 15(9), 1347.
- Koes, D. R., & Camacho, C. J. (2012). ZINCPharmer: pharmacophore search of the ZINC database. *Nucleic acids research*, 40(W1), W409-W414.
- Koopmans, T. (1934). Über die Zuordnung von Wellenfunktionen und Eigenwerten zu den einzelnen Elektronen eines Atoms. *Physica*, 1(1-6), 104-113.
- Kumalo, H., & Soliman, M. E. (2016). Per-residue energy footprints-based pharmacophore modeling as an enhanced in silico approach in drug discovery: a case study on the identification of novel β -secretase1 (BACE1) inhibitors as anti-Alzheimer agents. *Cellular and Molecular Bioengineering*, 9(1), 175-189.
- Ma, W., Li, S., Ma, S., Jia, L., Zhang, F., Zhang, Y., . . . Lu, X. (2016). Zika virus causes testis damage and leads to male infertility in mice. *Cell*, 167(6), 1511-1524. e1510.
- Millichap, J. G. (2016). Zika virus infection and microcephaly. *Pediatric neurology briefs*, 30(1), 8.
- Miner, J. J., & Diamond, M. S. (2016). Understanding how Zika virus enters and infects neural target cells. *Cell stem cell*, 18(5), 559-560.
- Mlakar, J., Korva, M., Tul, N., Popović, M., Poljšak-Prijatelj, M., Mraz, J., Fabjan Vodusek, V. (2016). Zika virus associated with microcephaly. *New England Journal of Medicine*, 374(10), 951-958.
- Morris, G. M., Goodsell, D. S., Halliday, R. S., Huey, R., Hart, W. E., Belew, R. K., & Olson, A. J. (1998). Automated docking using a Lamarckian genetic algorithm and an empirical binding free energy function. *Journal of computational chemistry*, 19(14), 1639-1662.
- Pandey, M., Muthu, S., & Gowda, N. N. (2017). Quantum mechanical and spectroscopic (FT-IR, FT-Raman, ¹H, ¹³C NMR, UV-Vis) studies, NBO, NLO, HOMO, LUMO and Fukui function analysis of 5-Methoxy-1H-benzo [d] imidazole-2 (3H)-thione by DFT studies. *Journal of Molecular Structure*, 1130, 511-521.
- Pettersen, E. F., Goddard, T. D., Huang, C. C., Couch, G. S., Greenblatt, D. M., Meng, E. C., & Ferrin, T. E. (2004). UCSF Chimera—a visualization system for exploratory research and analysis. *Journal of computational chemistry*, 25(13), 1605-1612.
- Sahoo, M., Lingaraja Jena, S. D., & Kumar, S. (2016). Virtual screening for potential inhibitors of NS3 protein of Zika virus. *Genomics & informatics*, 14(3), 104.
- Shapshak, P., Sinnott, J. T., Somboonwit, C., & Kuhn, J. H. (2015). *Global Virology I-Identifying and Investigating Viral Diseases*: Springer.

- Shawan, M., Hossain, M. M., Hasan, M. A., Hasan, M. M., Parvin, A., Akter, S., . . . Rahman, M. N. (2015). Design and prediction of potential RNAi (siRNA) molecules for 3'UTR PTGS of different strains of zika virus: a computational approach. *Nat. Sci*, 13(2), 37-50.
- Singh, R. K., Dhama, K., Malik, Y. S., Ramakrishnan, M. A., Karthik, K., Tiwari, R., . . . Joshi, S. K. (2016). Zika virus—emergence, evolution, pathology, diagnosis, and control: current global scenario and future perspectives—a comprehensive review. *Veterinary Quarterly*, 36(3), 150-175.
- Tang, H., Hammack, C., Ogden, S. C., Wen, Z., Qian, X., Li, Y., . . . Lee, E. M. (2016). Zika virus infects human cortical neural progenitors and attenuates their growth. *Cell stem cell*, 18(5), 587-590.
- Wang, Y., Xing, J., Xu, Y., Zhou, N., Peng, J., Xiong, Z., . . . Chen, K. (2015). In silico ADME/T modelling for rational drug design. *Quarterly reviews of biophysics*, 48(4), 488-515.
- Waring, M. J. (2010). Lipophilicity in drug discovery. *Expert Opinion on Drug Discovery*, 5(3), 235-248.
- Wu, C.-F., Wang, S.-H., Sun, C.-M., Hu, S.-T., & Syu, W.-J. (2003). Activation of dengue protease autocleavage at the NS2B–NS3 junction by recombinant NS3 and GST–NS2B fusion proteins. *Journal of virological methods*, 114(1), 45-54.
- Yang, W., & Parr, R. G. (1985). Hardness, softness, and the Fukui function in the electronic theory of metals and catalysis. *Proceedings of the National Academy of Sciences*, 82(20), 6723-6726.
- Yuan, S., Chan, J. F.-W., den-Haan, H., Chik, K. K.-H., Zhang, A. J., Chan, C. C.-S., . . . Zhu, Z. (2017). Structure-based discovery of clinically approved drugs as Zika virus NS2B-NS3 protease inhibitors that potently inhibit Zika virus infection in vitro and in vivo. *Antiviral research*, 145, 33-43.